Three-elemental models for the positive electrode of the lead/acid cell
II. Simulation results

R. R. Nilson and R. I. Chaplin
Department of Production Technology, Massey University, Private Bag, Palmerston North (New Zealand)

(Received June 17, 1992)

Abstract

Results for the discharge capacity, discharge surface area and charge surface area elemental models are reported. Where possible, model parameters are determined from experimental studies applicable to a practical lead/acid cell.

The discharge capacity model gave a capacity of 0.52 times the theoretical value. This compares well with a practical cell if the preferential discharge at the plate surface is taken into account.

The simple discharge surface area model gave a linear variation with charge state between the charge and discharge surface area parameter values used.

The charge surface area model showed an actual PbO_2 surface area that increased steadily with charge state between the same values as the discharge surface area model. The $PbSO_4$ surface area showed a gradual decrease until a charge state of about 0.8 and, thereafter, a rapid decrease to zero. The effective PbO_2 surface area followed the trend of the $PbSO_4$ surface area. The total ($PbO_2 + PbSO_4$) surface area variation with charge state was consistent with trends shown in the limited experimental data available. Acid concentration and geometric parameter values had a negligible influence on the model results. Increasing charge current caused a small decrease in the effective PbO_2 area result.

Introduction

Elemental models for the discharge capacity, discharge surface area and charge surface area of a small volume of the active mass (AM) in the positive electrode of the lead/acid battery have been set out previously [1]. The elemental models together with an aggregate model [2] can be used to simulate the complete positive electrode system. This paper gives the results of computer simulation based on the elemental models.

The fixing of model parameters is discussed first. The straightforward results for the discharge capacity and discharge surface area models are then given. The remainder of the paper concerns the more complex data for the charge surface area model.

Fixing model parameters, constants and variables

The elemental models have structural parameters determined by the AM. The charge surface area model also has geometric constants (set to likely values) and independent variables of charge current and acid concentration.

0378-7753/93/$6.00

Structural parameters

The microstructure solution volume and total surface area at full charge and discharge are the structural parameters determined by the AM. These are specified as gram equivalent quantities (quantities associated with one gram of fully-charged PbO_2).

The structural parameters were estimated from published data for AM undergoing discharge [3]. These data were adopted since the AM composition closely matched that of cells used in experiments associated with the development of the elemental models. The volume change involved was 0.044×10^{-6} m^3 per gram of discharged AM. When corrected for the weight of $PbSO_4$ present, this gave a gram equivalent value of 0.050×10^{-6} m^3 g^{-1}. The full discharge surface area also required weight correction to give an equivalent gram value. The full discharge PbO_2 surface area of 1.57 m^2 g^{-1} was obtained by halving the total corrected value to account for the contribution of the $PbSO_4$ surface [1]. The full charge surface area of 3.60 m^2 g^{-1} was obtained directly from the adopted AM data.

Geometric constants for the charge surface area model

PbO_2 is represented by a number of growing lobes on a PbO_2 sphere contained in a box of $PbSO_4$. This representation involves geometric constants for the sphere surface factor, lobe surface factor and the number of lobes per sphere.

The surface area factors were fixed for each simulation. The sphere surface factor was kept within the range 1.2 to 1.5 of a normal spherical surface. This is consistent with the discharge model description which suggests high surface area features are largely removed by the discharge process [1]. The lobe surface factor was kept within the range 1.2 to 2 of a normal cylindrical surface. This acknowledges that the lobe structures grow in irregular high surface area forms.

The number of lobes per sphere was selected by iteration to give a result for the equivalent gram surface area at full charge that was equal to the value for the adopted AM.

Variables for the charge surface area model

Simulations were performed with a number of constant current charges in the range 62.5×10^{-3} to 625×10^{-3} A g^{-1}.

Simulations were also conducted with a number of constant acid concentration charges in the range 1000 to 10 000 mol m^{-3}. Both the lead-ion concentration and the diffusion coefficient depend on the acid concentration and were taken from tabulated data [4].

Results for the discharge capacity model

The discharge capacity is calculated from the micropore solution volume parameter. For the adopted AM, this was 0.05×10^{-6} m^3 g^{-1} and gave a discharge capacity of 418 A s g^{-1} or an AM utilization of 0.52 times the theoretical value. In the deep discharge of a traction cell, typically only the outer half of the plate is fully discharged because of preferential discharge at the plate surface. The average utilization factor for the entire plate is typically 0.25. This corresponds to a utilization factor in the full discharged AM of 0.50 which is close to the model value.

Results for the discharge surface area model

The parameters for the discharge surface area model are the full charge and the full discharge PbO_2 surface area. For the adopted AM, these were 3.60 and 1.57 m^2 g^{-1}, respectively. The simple discharge surface area model gives a linear variation with charge state between these extreme values.

Results for the charge surface area model

The structural parameters for the charge surface area model are the same as those used for the other two models. Other constants and independent variables are altered in successive simulations to assess the response of the model.

Standard results

Standard results are for a 62.5×10^{-3} A g^{-1} (approximately the 1 h rate) constant current and 5.0×10^{3} mol m^{-3} constant concentration charge. The sphere and lobe surface factors are 1.2 and 2.0, respectively. Figure 1 shows the development of surface area during charge. The vertical axis gives the equivalent gram surface area for the four area quantities (i.e., $PbSO_4$, actual PbO_2, $PbSO_4+PbO_2$, and effective PbO_2) defined by the model. The horizontal axis gives the charge state from fully discharged to fully charged (0 to 1, respectively).

It can be seen that the $PbSO_4$ surface area slowly reduces throughout most of the charge and then falls rapidly towards the end of charge. This behaviour is consistent with the gradual consumption of solid $PbSO_4$. Towards the end of charges, this will leave relatively low-volume, high-surface area particles. The rapid reduction in surface area at the end of charge is consistent with the consumption of particles of this type.

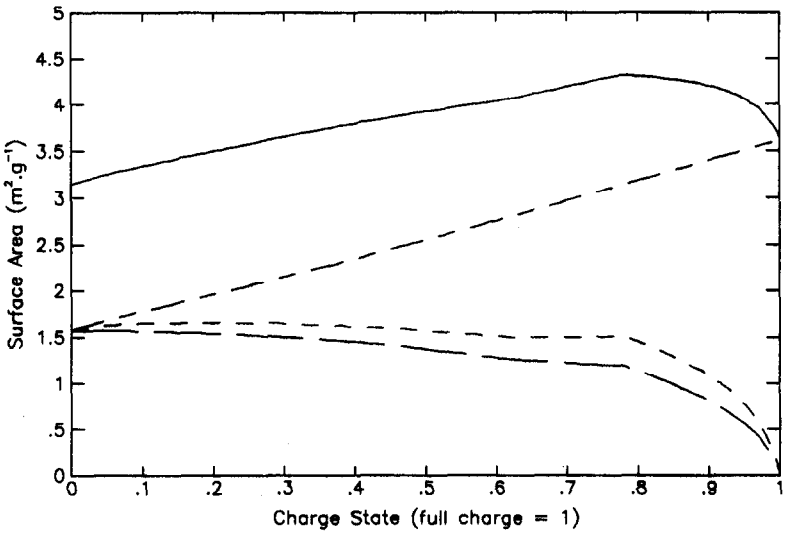

Fig. 1. Charge surface area development—standard case: (solid) PbO_2+PbSO_4 surface; (large dash) $PbSO_4$ surface; (small dash) effective PbO_2 surface, and (large + small dash) PbO_2 surface. Charge current: 62.5×10^{-3} A g^{-1} (~1 h rate), acid concentration: 5.0×10^{3} mol m^{-3}.

The PbO_2 surface increases throughout the charge. The increase is slightly more marked towards the end of charge. This is consistent with the development of lobes that grow more rapidly in length as the surrounding $PbSO_4$ retreats more rapidly into the corners of the sphere/box geometry towards the end of charge. The effective PbO_2 surface follows above the $PbSO_4$ surface throughout most of the charge. This is consistent with the controlling effect of the supply of ions from the $PbSO_4$ surface to the adjacent PbO_2 surface. The effective PbO_2 surface falls to zero at the end of charge as the reducing $PbSO_4$ surface and associated ion supply vanishes. The total ($PbSO_4 + PbO_2$) solid phase surface area increases for most of the charge but decreases towards the end of charge.

The profiles of lobes at various stages of the surface area development are given in Fig. 2. The vertical axis gives the lobe radius normalized to the maximum possible radius. The horizontal axis gives the lobe length normalized to the radial distance from the sphere surface to the box corner within the sphere/box geometry. The horizontal axis is an axis of rotation through the centre of the lobe.

It can be seen that the lobes in Fig. 2 have grown as pointed tent-like shapes. As the charge proceeds, the shapes get proportionately longer. This indicates that lobe growth is favoured near the retreating $PbSO_4$ surface (near the lobe point) as the charge proceeds. This is consistent with an increasing gradient in Pb^{2+} ion concentration caused by the increasing current density throughout the charge. The overall effect is that lobes, that continue to grow until the end of charge, have a larger surface area than those fully formed at an earlier stage. It must be remembered, when examining the lobe profiles, that the vast majority of lobes in the fully-charged AM will be those formed during the early part of the charge. Only a few lobes would be accompanied by adjacent $PbSO_4$ and therefore able to continue to grow during the latter stages of the charge. Because of this, the surface area of lobes at charge states approaching unity have only a minor effect on the overall PbO_2 surface area.

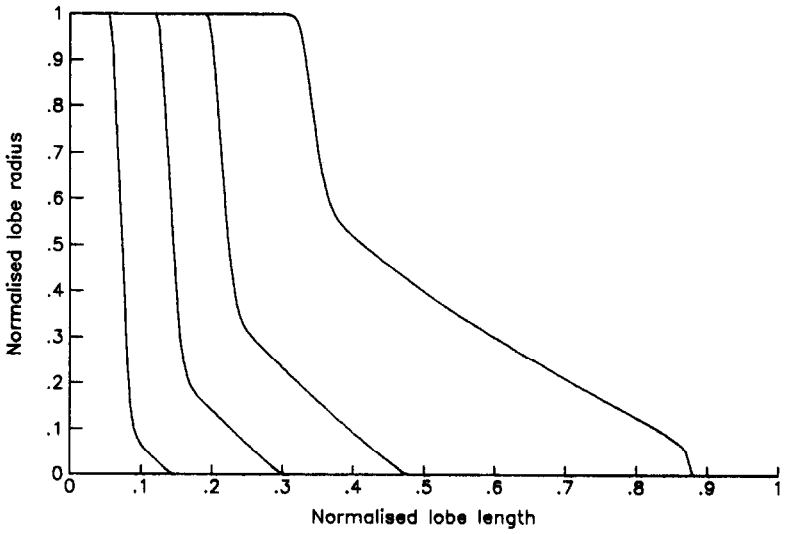

Fig. 2. Lobe profiles—standard case. Charge state for profiles from left to right: 0.25, 0.5, 0.75 and 0.99. Charge current: 62.5×10^{-3} A g^{-1} (~1 h rate), acid concentration: 5.0×10^3 mol m^{-3}.

Results for various charge currents

Figures 3 and 4 give the results of the charge surface area model where the charge current is varied. The other factors are the same as in the standard case. From Fig. 3, it can be seen, that at all but very high currents, the actual PbO_2 surface area is almost the same as the low current case. That is, it is virtually independent of current. At very high currents, the surface area at the end of charge rapidly exceeds that of the low current case. The reason for the increase in surface area at high currents can be seen in Fig. 4. At moderate and high currents, the lobes develop a radial shelf of large surface area near the retreating $PbSO_4$ surface. At moderate currents, this shelf is only a minor feature on the few lobes growing at the very end of charge. At high currents, it is more extensive, forms earlier and on more lobes than at moderate currents. No growth of this type is evident until the charge is more than 75% complete. The development of rapidly-growing finely-structured lobes as seen here is typical of the dendritic growth that occurs when precipitation reactions are concentrated onto a small area. This is expected here as the Pb^{2+} ion concentration gradient increases with increasing current density and ions are only available very near the retreating $PbSO_4$ surface. The effective PbO_2 surface area seen in Fig. 3 reduces as the current increases to medium and high values. This effect is also expected as the Pb^{2+} ion concentration gradient increases with increasing current density, and restricts the supply of ions to the lower regions of the growing lobes. The effect is, however, counteracted to some extent by the growth of 'shelves' of large surface area near the retreating $PbSO_4$ as already discussed. The overall result is that the reduction in the effective surface area with increasing current is small.

Results for various acid concentrations

Figures 5 and 6 give the results for the charge surface area model where the acid concentration is varied. The other factors are the same as in the standard case.

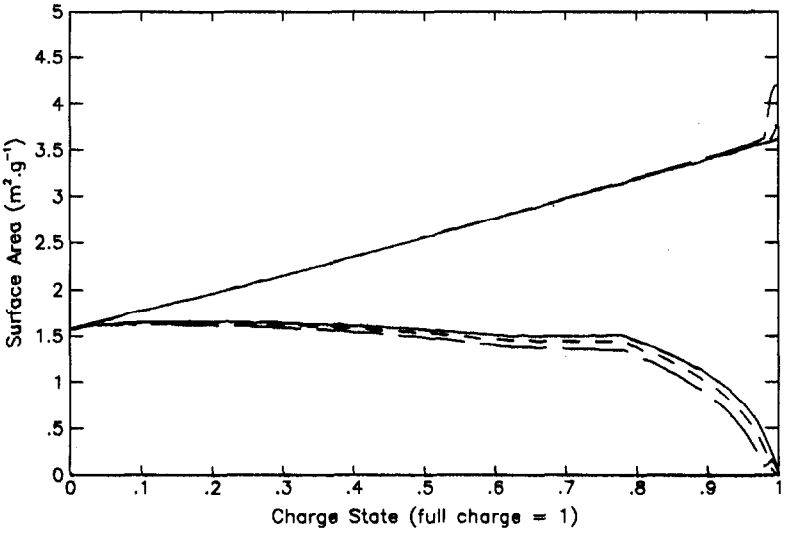

Fig. 3. Charge surface area for various currents: (top curves) actual PbO_2 surface; (bottom curves) effective PbO_2 surface; (solid) current 62.5×10^{-3} A g^{-1} or less (~1 h rate); (small dash) current 312.5×10^{-3} A g^{-1}, and (large dash) current 625.0×10^{-3} A g^{-1}; acid concentration: 5×10^3 mol m^{-3}.

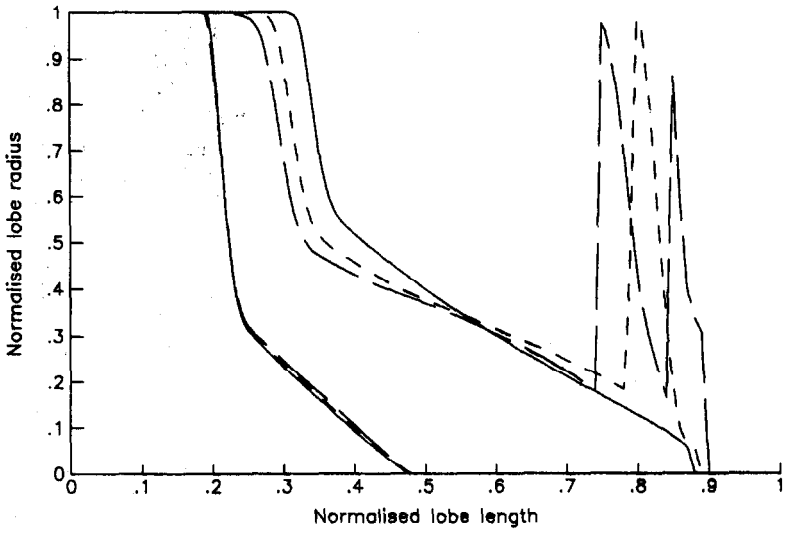

Fig. 4. Lobe profiles for various currents: charge state of profiles on left: 0.75; charge state of profile on right: 0.99; (solid) current 62.5×10^{-3} A g^{-1} (~1 h rate); (small dash) current 312.5×10^{-3} A g^{-1}; (large dash) 625.0×10^{-3} A g^{-1}; acid concentration: 5×10^{3} mol m^{-3}.

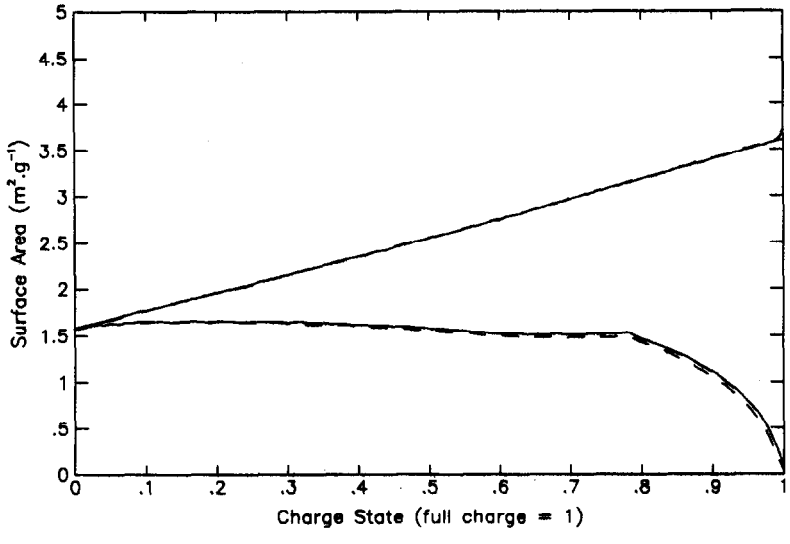

Fig. 5. Charge surface area for various acid concentrations: (top curves) actual PbO_2 surface; (bottom curves) effective PbO_2 surface; (solid) concentration 1000 mol m^{-3} or less, and (small dash) concentration 10 000 mol m^{-3}. Charge current in all cases: 62.5×10^{-3} A g^{-1} (~1 h rate).

Figure 5 shows that both the actual and effective PbO_2 surface areas are only slightly effected by acid concentration. Even then, the largest effect is associated with a very concentrated acid solution which is unlikely to be found in a practical cell. Figure 6 shows the lobe profiles for various acid concentrations. The appearance of radial

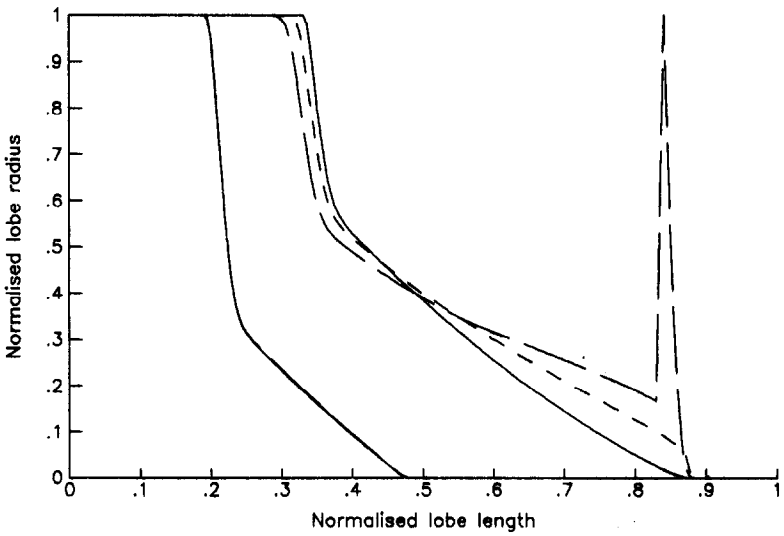

Fig. 6. Lobe profiles for various acid concentrations: charge state of profiles on left: 0.75; charge state of profiles on right: 0.99; (solid) concentration 1000 mol m^{-3} or less; (small dash) concentration 5000 mol m^{-3}, and (large dash): 10 000 mol m^{-3}. Charge current in all cases: 62.5×10^{-3} A g^{-1} ($\sim$1 h rate).

shelves can be seen at high acid concentrations. These shelves are always minor features on the few growing lobes at the end of charge. The lobes are again expected as the Pb^{2+} ion concentration gradient increases with increasing acid concentration. This is because the Pb^{2+} ion diffusion coefficient falls as the acid concentration increases.

Results for various geometric constants

Figures 7 and 8 present the results of the charge surface area model where the geometric constants are varied. The other factors are the same as in the standard case. The actual and effective surface area development, shown in Fig. 7, is virtually independent of the particular values chosen. This is a surprising result in the light of the lobe profiles shown in Fig. 8. Here it can be seen that the lobe surface factor has little effect on the lobe profiles. The lobe profiles are, however, strongly dependent on the sphere surface factor. This is a consequence of a change in the proportions of the sphere/box geometry that is dictated by this constant. The surprising point is that the different lobe shape and the change in sphere/box proportions interact to give an equivalent gram area that remains virtually independent of the sphere surface factor. For the purpose of defining the effective surface area distribution results, the minor dependence seen above eliminates the need for precise estimates of the geometric constants. This is fortunate since these constants cannot be easily defined from experimental studies.

The effective surface area and the aggregate model

The incorporation of the charge surface area model into the aggregate model for the complete positive electrode system will now be considered. Here, it is only the effective PbO_2 surface area that is required. The results above show that this is virtually independent of acid concentration and geometric constants. This means the deter-

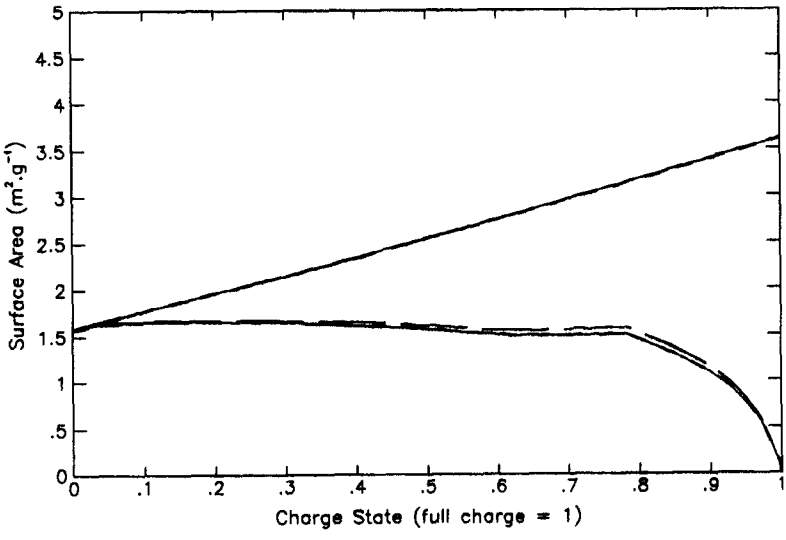

Fig. 7. Charge surface area for various geometric constants: (top curves) actual PbO_2 surface; (bottom curves) effective PbO_2 surface; (solid) $f_0=1.2$, $f_v=2$, $n_v=4$; (large dash) $f_0=1.5$, $f_v=2$, $n_v=7$, and (small dash) $f_0=1.2$, $f_v=1.2$, $n_v=11$, where f_0 and f_v are the sphere and lobe surface factors, respectively, and n_v is the number of lobes. Charge current in all cases: 62.5×10^{-3} A g^{-1}.

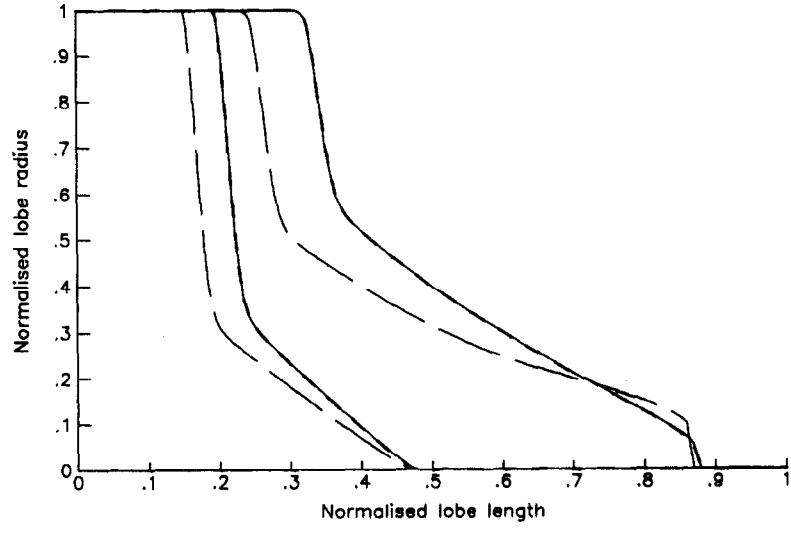

Fig. 8. Lobe profiles for various geometric constants: charge state of profiles on left: 0.75; charge state of profiles on right: 0.99; (solid) $f_0=1.2$, $f_v=2$, $n_v=4$; (large dash) $f_0=1.5$, $f_v=2$, $n_v=7$ and (small dash) $f_0=1.2$, $f_v=1.2$, $n_v=11$, where f_0 and f_v are the sphere and lobe surface factors, respectively, and n_v is the number of lobes. Charge current in all cases: 62.5×10^{-3} A g^{-1}.

mination of the effective PbO_2 surface area can be taken as a function of charge state and instantaneous current only.

To implement this simplification, the effective PbO_2 results for low and high currents were fitted to polynomial forms of charge state. The required effective surface area was then defined by fixing the charge state and performing a linear interpolation between the two curves based on the instantaneous current.

Discussion of the charge surface area model

In this results above, the quantitative model performance has been shown to be consistent with the qualitative descriptions upon which the model is based. At this point, attention will be given to comparing the model results with the rather limited data available from experimental studies.

Dimensions of structural features

The model represents the dimensions and structure of a typical PbO_2 crystallite within the microstructure of the AM. At full charge, the overall dimensions are those of the sphere/box arrangement. Within these dimensions, the crystallite has many lobes (edges and spires) surrounding a solid base structure that is slightly larger than the sphere of the sphere/box arrangement. This representation can be compared with experimental observations of AM microstructure. The model dimensions are 0.119×10^{-6} and 0.190×10^{-6} m for the sphere radius and half the box width, respectively. A micrograph of fully charged AM similar to the adopted AM [3] shows a wide range of crystallites within the structure that vary in radius from about 0.25 to 0.03×10^{-6} m. These dimensions compare well with the dimensions of the model given above.

Trends in total surface area variation

The charge surface area model gives the total ($PbSO_4 + PbO_2$) surface area variation with charge state. Typical results for the adopted AM are given in Fig. 1. Experimental measurements of the total surface per gram at four points in a charge cycle have been made [5]. These points were converted to gram equivalent values and are marked as circles in Fig. 9. Both the model and experimental results show a significant increase in surface area in the first half of the charge cycle, and little overall increase in surface area thereafter. Two main differences are also seen. First, the increase in the initial experimental surface area is very rapid compared with that for the model. In the experimental work, it is suggested that $PbSO_4$ encapsulation of PbO_2 depresses the surface area measurement value at full discharge. This means that the true experimental surface area value at full discharge should be adjusted upwards toward the model value. Second, the final experimental surface area shows no change compared with a declining value for the model. In fact, this is an assumed form in the absence of additional measurements in this region.

Direct numerical comparison of the model and experimental results is not valid since the AM is quite different. The surface area in the experimental AM was 6.40 and 1.25 $m^2\ g^{-1}$ and in the adopted AM 3.60 and 2.75 $m^2\ g^{-1}$ for the full charge and full discharge areas, respectively. Nevertheless, discounting numerical values, some similar trends were observed.

A direct comparison of total surface area variation

An alternative approach was used to give a more direct comparison between the model and experimental results where the model parameters were redefined from data

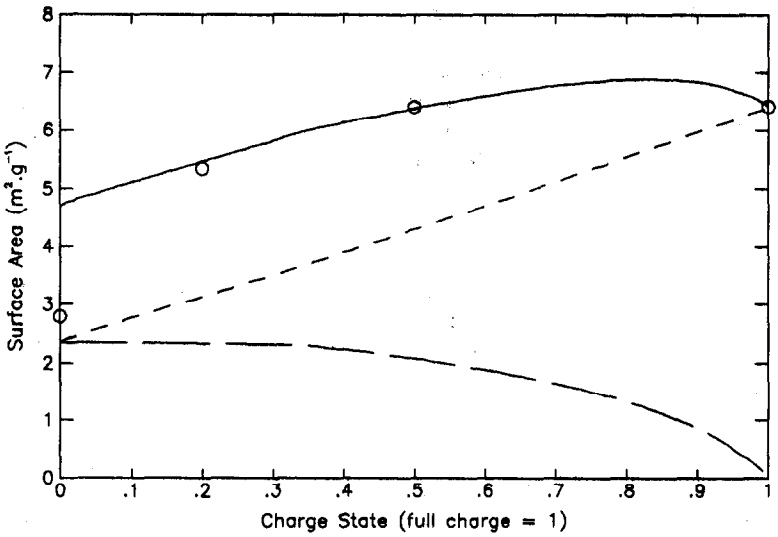

Fig. 9. Model and experimental charge surface area: (solid) model $PbSO_4 + PbO_2$ surface; (small dash) model PbO_2 surface; (large dash) model $PbSO_4$ surface, and (O) experimental $PbSO_4 + PbO_2$ surface[a]. Model charge current: 31.2×10^{-3} A g^{-1} ($\sim$2 h rate), model acid concentration: 5.0×10^3 mol m^{-3}.
[a]From ref. 5 corrected for $PbSO_4$ weight.

for the experimental AM. The charge surface area parameters are given above and the microstructure solution volume was 0.037×10^{-6} m^3 g^{-1}. New simulations were performed with a sphere and lobe surface factor of 1.2 and 2, respectively, and estimates for the PbO_2 surface area at full discharge and the number of lobes per sphere. The estimated parameters were changed by iteration until the model area results agreed with the corrected full and half charge experimental values. The experimental values at less than half charge were not taken into account because of the undetermined amount of encapsulated surface involved. The model results obtained in this way are given together with the experimental results in Fig. 9. It can be seen that a considerable upward adjustment of the experimental values in the initial part of the charge is still required to align the two results. Without further experimental work, it cannot be determined whether or not the argument of encapsulated PbO_2 justifies this adjustment.

No experimental data exist to validate the effective PbO_2 surface area results.

Conclusions

Successful computer simulations of discharge capacity, discharge surface area and charge surface area have been performed using elemental models. The model parameters were defined using data applicable to a practical lead/acid cell.

The discharge capacity model result compared well with that obtained in practice. The discharge surface area model gave a simple and convenient result for use with an aggregate model of the complete electrode system [2].

The charge surface area model results showed little variation with either acid concentration or geometric constants and could be adequately represented as functions

of charge state and current. The results were in agreement with experimental studies under all but very deep discharge conditions. At deep discharge, the effect of surface area masking due to void and PbO_2 encapsulation by $PbSO_4$ may be a factor. The charge surface area model provides a framework, based on the AM structure and electrochemistry, that defines the effective charge surface needed in the aggregate model.

Some measure of the performance of the elemental models can be made by comparing the aggregate model and practical cell results [6].

References

1 R. R. Nilson, *J. Power Sources, 41* (1993) 1–12.
2 R. R. Nilson, *J. Power Sources, 41* (1993) 25–37.
3 D. Pavlov and E. Bastavelova, *J. Electrochem. Soc., 133* (1986) 241.
4 V. Danel and V. Plichon, *Electrochim. Acta, 27* (1982) 771.
5 P. Ekdunge and D. Simonsson, *J. Electrochem. Soc., 132* (1985) 252.
6 R. R. Nilson and R. I. Chaplin, *J. Power Sources, 41* (1993) 39–53.